

# Inference for a generalised stochastic block model with unknown number of blocks and non-conjugate edge models

Matthew Ludkin<sup>a</sup>

<sup>a</sup>*Mathematics and Statistics, Lancaster University, Lancaster, United Kingdom, LA1 4YW.*

---

## Abstract

The stochastic block model (SBM) is a popular model for capturing community structure and interaction within a network. Network data with non-Boolean edge weights is becoming commonplace; however, existing analysis methods convert such data to a binary representation to apply the SBM, leading to a loss of information. A generalisation of the SBM is considered, which allows edge weights to be modelled in their recorded state. An effective reversible jump Markov chain Monte Carlo sampler is proposed for estimating the parameters and the number of blocks for this generalised SBM. The methodology permits non-conjugate distributions for edge weights, which enable more flexible modelling than current methods as illustrated on synthetic data, a network of brain activity and an email communication network.

*Keywords:* network, stochastic block model, statistical analysis of network data, non-conjugate analysis

---

## 1. Introduction

Statistical analysis of networks has seen much growth in recent years with the increasing availability of network data. In this paper, a network consists of a set of nodes, which can form pairwise interactions. Each possible interaction is referred to as an *edge*, with the value of that interaction called an *edge weight*.

The aim of statistical network modelling is to describe the edge weights with a probabilistic model, potentially performing inference for model parameters. Such models include the exponential random graph (Snijders et al., 2006), the class of latent space models (Hoff et al., 2002) and the stochastic block model (SBM) (Frank and Harary, 1982; Holland et al., 1983). In the classic SBM, the set of nodes is partitioned into *blocks* such that the edge weight between two nodes depends on their block memberships. There is a rich literature on the SBM including both Bayesian and frequentist treatments. Extensions to the SBM include restricting the SBM to only within-block and between-block edge-weight distributions in the affiliation network (Snijders and Nowicki, 1997; Nowicki and Snijders, 2001; Copic et al., 2009), multiple-block memberships in the mixed-membership SBM (Airoldi et al., 2008), degree-corrected SBM (Karrer and Newman, 2011), and the infinite relational model (IRM), (Kemp et al., 2006) where the number of blocks is treated as unknown. For a thorough review of the SBM and inference methods, see Matias and Robin (2014).

---

*Email address:* m.ludkin1@lancaster.ac.uk (Matthew Ludkin)

18 This paper considers two extensions to the SBM: (i) modelling general edge weights (*i.e.* non-  
19 binary interaction data) and (ii) estimating the number of blocks. Previous authors have attempted  
20 extension (i) with a weighted or valued network (Jiang et al., 2009; Mariadassou et al., 2010;  
21 Ambroise and Matias, 2012) or considering a time-series of edge weights (Matias and Miele, 2017;  
22 Xin et al., 2017; Ludkin et al., 2018). Multiple methods have been considered for extension (ii); these  
23 fall into two main approaches: (a) a post-hoc analysis of multiple model fits using model selection  
24 techniques, and (b) treating the number of blocks as a random variable. Approach (a) includes  
25 likelihood-based methods using the Bayesian information criteria and its derivatives (Daudin et al.,  
26 2008; Latouche et al., 2012; Wang et al., 2017; Saldaña et al., 2017), information-based methods  
27 using minimum description lengths (Peixoto, 2013), sequential testing by embedding successive  
28 block models with an increasing number of blocks (Lei, 2016) and cross-validation (Chen and Lei,  
29 2016). Approach (b) is achieved in a Bayesian framework by setting a prior for the number of  
30 blocks. Geng et al. (2019) use a mixture of finite mixtures representation, while the IRM (Mørup  
31 and Schmidt, 2013) uses a Chinese Restaurant Process (CRP) (Gershman and Blei, 2012).

32 Some authors (Mørup et al., 2011; Mørup and Schmidt, 2012, 2013; McDaid et al., 2013) have  
33 considered both extensions (i) and (ii) and posited collapsed Gibbs samplers to perform inference on  
34 the number of blocks, node membership and edge-weight model parameters. However, all of these  
35 methods require a conjugate model for the edge-weight distributions. This article aims to achieve  
36 both extensions by generalising the SBM to arbitrary edge-weight distributions and modelling  
37 the number of blocks in one Bayesian framework *without* the restriction of conjugate edge-weight  
38 distributions. This is highlighted in Section 5.2 where a negative binomial model is applied to the  
39 edge weights within an email network. Such a model cannot be applied using existing methodology  
40 since no conjugate prior distribution exists for the negative binomial with both parameters unknown.  
41 This approach greatly broadens the applicability of the general stochastic block model to network  
42 data with non-conjugate edge-weight distributions.

43 The proposed methodology to perform inference is a Markov chain Monte Carlo sampler which  
44 provides samples from the posterior distribution of the block parameters, block memberships and  
45 number of blocks. The sampling algorithm is inspired by Green and Richardson (2001) – a reversible  
46 jump Markov chain Monte Carlo (RJMCMC) (Green, 1995) scheme using split and merge proposals  
47 to explore the posterior by either combining two blocks, or splitting a block into two. Nobile and  
48 Fearnside (2007); McDaid et al. (2013) make use of a split-merge proposal, although due to the  
49 conjugate models considered, they do not require parameter values. The difficulty in designing  
50 an effective split-merge algorithm rests on ensuring that parameter values are “matched” when  
51 changing dimension. Previous authors have proposed sampling algorithms, such as the collapsed  
52 Gibbs sampler of McDaid et al. (2013) – for a given node, the posterior probability of belonging to  
53 a given block is computed with all other parameters fixed. Under the collapsed regime, assigning  
54 a node to a new block is simple, since the parameters have been integrated from the model. In  
55 the case of non-conjugate mixture models, the parameters are required to evaluate the likelihood  
56 of such a re-assignment; this added complexity can be handled within a full RJMCMC scheme as  
57 described in Section 3.

58 The remainder of the paper is organised as follows: in Section 2, the specifics of the generalised  
59 SBM are presented. Section 3 introduces the split-merge sampling algorithm. In Section 4, the  
60 sampler is applied to simulated data, whilst in Section 5, the split-merge sampler is used to analyse  
61 some real network data. Finally, closing remarks and extensions to the model and sampler are  
62 discussed in Section 6.

63 **2. A generalisation of the stochastic block model**

64 This section describes the stochastic block model and details the generalisation to arbitrary  
 65 edge-weight distributions for network data.

66 Mathematically, a network is represented as a *weighted graph*  $\mathcal{G} = (\mathcal{V}, \mathcal{E}, \mathcal{W})$  where  $\mathcal{V}$  is the set of  
 67 nodes,  $\mathcal{E} \subseteq \mathcal{V} \times \mathcal{V}$  is the set of edges and  $\mathcal{W}$  is the set of edge weights. This paper uses the shorthand  
 68  $ij \in \mathcal{E} \implies (i, j) \in \mathcal{E}$ . The *weight* of edge  $ij$  is denoted by  $W_{ij} \in \mathcal{W}$ . To simplify exposition, it  
 69 is assumed that all edge weights are observed, *i.e.*  $\mathcal{E} = \mathcal{V} \times \mathcal{V}$  and  $W_{ij} \in \mathcal{W}$  for all  $ij \in \mathcal{E}$ . In this  
 70 way, an un-weighted graph  $\mathcal{G} = (\mathcal{V}, \mathcal{E})$  can be viewed as a weighted graph  $\mathcal{G}' = (\mathcal{V}, \mathcal{E}', \mathcal{W}')$  with  
 71  $\mathcal{E}' = \mathcal{V} \times \mathcal{V}$ ,  $W'_{ij} = 1$  if  $ij \in \mathcal{E}$  and  $W'_{ij} = 0$  otherwise. In the case where the network contains  
 72 directed edges, the set  $\mathcal{E}$  consists of ordered pairs such that  $(i, j) \neq (j, i)$ .

73 The canonical SBM (Holland et al., 1983; Fienberg et al., 1985; Wasserman and Anderson, 1987)  
 74 can be viewed as such a weighted graph with  $W_{ij} \in \{0, 1\}$ , a fixed number of nodes ( $|\mathcal{V}| = N$ ) and  
 75  $K$  blocks. The nodes are partitioned into blocks, with each node belonging to only one block. Let  
 76  $\mathbf{Z}$  be the block indicator matrix with  $Z_{ik} = 1$  if node  $i$  belongs to block  $k$  and 0 otherwise. As such,  
 77  $\mathbf{Z}_i$  is a one-of- $K$  indicator vector. It is assumed that  $\mathbf{Z}_i$  is drawn from a multinomial distribution  
 78 with parameter  $\boldsymbol{\rho}$ , a probability vector of length  $K$  which governs the block memberships. The prior  
 79 probability that a node belongs to block  $k$  is given by  $\rho_k$ . Let  $\boldsymbol{\theta}$  be a  $K \times K$  matrix of edge-weight  
 80 parameters, such that  $\vartheta_{kl}$  is the probability that  $W_{ij} = 1$  between nodes  $i$  and  $j$  in blocks  $k$  and  
 81  $l$  respectively. Note  $\vartheta_{kl} = \mathbf{Z}_i^\top \boldsymbol{\theta} \mathbf{Z}_j$ . This model is summarised in Equation (1); first the nodes  
 82 are assigned to blocks, then – given these block memberships – the edge weights are drawn with  
 83 parameters depending on the block membership of the end nodes.

$$\begin{aligned} \mathbf{Z}_i | \boldsymbol{\rho} &\stackrel{\text{iid}}{\sim} \text{Multinomial}(\boldsymbol{\rho}), \\ W_{ij} | \boldsymbol{\theta}, \mathbf{Z} &\stackrel{\text{ind}}{\sim} \text{Bernoulli}(\mathbf{Z}_i^\top \boldsymbol{\theta} \mathbf{Z}_j). \end{aligned} \tag{1}$$

85 In full generality, there are  $K(K+1)/2$  free parameters in  $\boldsymbol{\theta}$  for an un-directed network (or  $K^2$   
 86 for a directed network). In the affiliation model (Snijders and Nowicki, 1997; Nowicki and Snijders,  
 87 2001; Copic et al., 2009),  $\boldsymbol{\theta}$  is restricted to two parameters, one each for between-block ( $\vartheta_{kl}, k \neq l$ )  
 88 and within-block ( $\vartheta_{kk}$ ) interactions.

89 In this article, a parameterisation between these two extremes is considered: let  $\theta_k$  be the  
 90 parameters governing edge weights between nodes belonging to block  $k$ , and a global parameter  
 91  $\theta_0$  for edge weights between nodes in different blocks. In this way, the number of parameters is  
 92  $K+1$ , and grows linearly in the number of blocks. This model is appropriate for networks where  
 93 between-block connections are relatively homogeneous; for example, in ecological contact networks,  
 94 where herds of animals remain close together for most of the time, with some interactions between  
 95 herds. Let  $\boldsymbol{\theta}$  be the matrix of parameters with  $\theta_{kk} = \theta_k$  and  $\theta_{kl} = \theta_0$  for  $k = 1, \dots, K, l \neq k$ , then  
 96 the quadratic form  $\mathbf{Z}_i^\top \boldsymbol{\theta} \mathbf{Z}_j$  picks the parameter governing the edge weight  $W_{ij}$ .

97 With this parameterisation, the classic SBM in Equation (1) is extended to allow the number  
 98 of blocks to be random and to model general edge weights, such as count or continuous data. Let  
 99  $G$  and  $G_0$  be the distribution on the edges-weights and parameters respectively. Prior parameters  
 100  $\boldsymbol{\alpha}$  are assigned to the block parameters  $\boldsymbol{\theta}$ . Since the number of blocks  $K$  is considered unknown,  
 101 a prior must be placed on both the number of blocks and block memberships. Let  $F$  be a joint  
 102 distribution for  $(K, \mathbf{Z})$  with parameters  $\gamma$  and  $\delta$  then the generalised form of the SBM considered  
 103 in this paper is:

$$K, \mathbf{Z} \sim F(\gamma, \delta),$$

$$\theta_k \stackrel{\text{ind}}{\sim} G_0(\boldsymbol{\alpha}), \quad (2)$$

$$W_{ij} | \boldsymbol{\theta}, \mathbf{Z} \stackrel{\text{ind}}{\sim} G(\mathbf{Z}'_i \boldsymbol{\theta} \mathbf{Z}_j).$$

105 This framework may be extended to an edge-weight distribution  $G$  with multiple parameters.  
 106 For example, if  $G$  represents the normal distribution, then  $\theta_k = (\mu_k, \sigma_k)$  represents the mean and  
 107 standard deviation of the edge weights in block  $k$ . In this case, an additional subscript is required  
 108 on  $\theta_k$  such that  $\theta_{kp}$  is the  $p^{\text{th}}$  parameter for block  $k$ . In the normal example, line 3 of Equation (2)  
 109 yields  $W_{ij} | \boldsymbol{\theta}, \mathbf{Z} \stackrel{\text{ind}}{\sim} \text{Normal}(\mathbf{Z}'_i \boldsymbol{\mu} \mathbf{Z}_j, \mathbf{Z}'_i \boldsymbol{\sigma} \mathbf{Z}_j)$ .

110 The choice of distributions for  $G$  and  $G_0$  is driven by the type of edge weight considered (*i.e.* edge  
 111 weights representing counts could be modelled using a Poisson distribution for  $G$ ). On the other  
 112 hand, there is flexibility for distribution  $F$ . As discussed in Geng et al. (2019), the popular choice  
 113 of the Chinese Restaurant Process (CRP) yields the undesirable property that large probability is  
 114 assigned to blocks with relatively few nodes. Indeed, Miller and Harrison (2018) show that using a  
 115 CRP prior on  $(K, \mathbf{Z})$  in mixture models leads to inconsistent estimation of the number of clusters,  
 116 even in the asymptotic regime when  $N$  tends to infinity. To circumvent this, Miller and Harrison  
 117 (2018) propose using the “mixture of finite mixtures approach” (MFM) where the number of blocks  
 118 has an explicit prior distribution. Let  $F_0$  be a distribution on  $\{1, 2, 3, \dots\}$  with parameter  $\delta$ , then  
 119 the prior for  $(K, \mathbf{Z})$  considered in the remainder of the paper is given in Equation (3):

$$K \sim F_0(\delta),$$

$$\rho | K \stackrel{\text{ind}}{\sim} \text{Dirichlet}(\gamma, K), \quad (3)$$

$$\mathbf{Z}_i | \boldsymbol{\rho} \stackrel{\text{ind}}{\sim} \text{Multinomial}(\boldsymbol{\rho}),$$

where  $\text{Dirichlet}(\gamma, K)$  is the symmetric Dirichlet distribution on the  $K - 1$  simplex. The *size* of  
 block  $k$  is the number of nodes whose block membership is  $k$  and is given by  $N_k = \sum_{i=1}^N Z_{ik}$ . Let  
 $\mathbf{N} = \{N_k : k = 1, \dots, K\}$  be the set of block sizes, then the distribution for  $\mathbf{N}$  under the CRP and  
 the MFM are:

$$p_{\text{CRP}}(\mathbf{N}) = \prod_{k=1}^K N_k^{-1} \quad \text{vs.} \quad p_{\text{MFM}}(\mathbf{N}) = \prod_{k=1}^K N_k^{\gamma-1}.$$

121 Notice that the MFM gives comparatively less probability mass to small blocks than the CRP. Also,  
 122 the distribution for the CRP is independent of  $\gamma$ . Thus, the MFM approach gives more control over  
 123 the prior block structure.

The parameter  $\boldsymbol{\rho}$  can be marginalised out of Equation (3) to obtain a prior density for block  
 memberships depending only on  $K$  and  $\gamma$  as such:

$$f(\mathbf{Z} | \gamma, K) = \int_{\boldsymbol{\rho}} f(\mathbf{Z} | \boldsymbol{\rho}) \pi_0(\boldsymbol{\rho} | \gamma) d\boldsymbol{\rho} = \int_{\boldsymbol{\rho}} \prod_{k=1}^K \rho_k^{N_k + \gamma - 1} \frac{\Gamma(K\gamma)}{\Gamma(\gamma)^K} d\boldsymbol{\rho} = \frac{\Gamma(K\gamma)}{\Gamma(\gamma)^K} \frac{\prod_{k=1}^K \Gamma(\gamma + N_k)}{\Gamma(K\gamma + N)},$$

since  $\sum_{k=1}^K N_k = N$  and where  $\Gamma(a) = \int_0^\infty x^{a-1} e^{-x} dx$  is the gamma function; this is referred to as the

Dirichlet-Multinomial distribution. Similarly, the conditional distribution for the block membership of node  $i$ , given  $K$  and the other block memberships  $\mathbf{Z}_{-i}$  is:

$$\begin{aligned} f(\mathbf{Z}_i|\mathbf{Z}_{-i}, K, \gamma) &= \frac{f(\mathbf{Z}|\gamma, K)}{f(\mathbf{Z}_{-i}|\gamma, K)} = \frac{\prod_{k=1}^K \Gamma(\gamma + N_k) \Gamma(K\gamma + N - \sum_{k=1}^K Z_{ik})}{\Gamma(K\gamma + N) \prod_{k=1}^K \Gamma(\gamma + N_k - Z_{ik})} \\ &= \frac{1}{K\gamma + N - 1} \prod_{k=1}^K \frac{\Gamma(\gamma + N_k)}{\Gamma(\gamma + N_k - Z_{ik})}, \end{aligned}$$

since  $\sum_{k=1}^K Z_{ik} = 1$  and  $x\Gamma(x) = \Gamma(x+1)$ . Therefore,

$$f(Z_{il} = 1|\mathbf{Z}_{-i}, K, \gamma) = \frac{\gamma + N_l - 1}{K\gamma + N - 1}.$$

124 In the remainder of this article, the generalised SBM (GSBM) used is:

$$\begin{aligned} K - 1 &\sim \text{Pois}(\delta), \\ \mathbf{Z}|K &\stackrel{\text{ind}}{\sim} \text{Dirichlet-Multinomial}(\gamma, K), \\ \boldsymbol{\theta}_k &\stackrel{\text{ind}}{\sim} G_0(\boldsymbol{\alpha}), \\ W_{ij}|\boldsymbol{\theta}, \mathbf{Z} &\stackrel{\text{ind}}{\sim} G(\mathbf{Z}'_i \boldsymbol{\theta} \mathbf{Z}_j), \end{aligned} \tag{4}$$

126 where  $G_0$  and  $G$  are specified by the modeller. The prior on  $(K, \mathbf{Z})$  will be referred to as the  
127 DMA( $\gamma, \delta$ ) (Dirichlet-Multinomial Allocation) prior. When a model  $G$  is defined, we refer to the  
128 specific form of the model as  $G$ -SBM.

### 129 3. Split-merge sampler

130 This section discusses the benefit of split-merge steps over Gibbs samplers for mixture models,  
131 describes the difficulty that arises when designing split-merge moves for block membership in the  
132 GSBM, and presents a split-merge RJMCMC sampler for the GSBM. This algorithm draws samples  
133 from the posterior distribution of  $(K, \mathbf{Z}, \boldsymbol{\theta})$ .

134 For models containing a mixture component (such as the block structure in [Mørup and Schmidt,](#)  
135 [2012; McDaid et al., 2013](#)) a Gibbs sampler can get stuck in local modes of the posterior. Consider  
136 two “true” blocks  $k$  and  $l$  with sizes  $N_k \geq N_l$  and a state  $s$  of a Gibbs sampler with a block  $k^s$   
137 consisting of all nodes in true blocks  $k$  and  $l$ . For the Gibbs sampler to separate the nodes in  $k^s$   
138 into blocks  $k$  and  $l$ , it will require at least  $N_l$  steps, each of which takes a node assigned to  $k^s$   
139 and assigns it to a new block  $l^s$ . Each of these moves is quite unlikely, especially if the parameters  
140  $\boldsymbol{\theta}_k, \boldsymbol{\theta}_l$  are close to  $\boldsymbol{\theta}_0$ . On the other hand, if all nodes could be moved at once, then the proposal  
141 would be more likely to be accepted. This is a common problem with Gibbs sampling algorithms:  
142 the one-at-a-time nature of the algorithm means large changes in posterior space are unlikely, even  
143 if the combined changes increase the posterior considerably. One way to address this is to use a  
144 split-merge sampler.

145 Split-merge samplers have been developed for general mixture models (Green and Richardson,  
146 2001), with emphasis on a mixture of normal densities. In a standard parametric mixture model,  
147 each component has a different form (either different distributions or different parameter values)  
148 and each data point is drawn from a component of the mixture. A split-merge sampler applied  
149 to such a data set explores the possible assignments of data points to components by successively  
150 proposing to either merge two components together or split one component in two. Care must be  
151 taken when designing such proposals: they must be an isomorphism and differentiable to ensure  
152 the validity of the underlying Markov chain. Furthermore, to be efficient, a proposed structure  
153 should have similar posterior support to the current structure to give a reasonable probability of  
154 acceptance. Notice that, since each data point belongs to one component, a split move which assigns  
155 a data point to a new cluster will be penalised by the prior on the number of components, but the  
156 likelihood will increase if the parameter for the new component is a good fit for the assigned data  
157 point. Compare this to the latent block membership of the GSBM: reassigning a node  $i$  to a new  
158 block *affects all nodes with an edge to  $i$* . This implies that the prior will penalise the split move  
159 for adding a block for the new node, and the likelihood will penalise based on the  $(N - 1)$  edge  
160 weights incident to  $i$ . Therefore, when considering split-merge samplers for the GSBM, multiple  
161 edge weights are affected by changing the block membership of one node; this fact complicates the  
162 design of a successful proposal.

163 The remainder of this section introduces the split-merge sampler for the GSBM. The sampler  
164 consists of four moves: re-sampling parameter values, splitting or merging blocks, reassigning nodes  
165 to the current set of blocks, and adding or deleting an empty block.

166 Let  $(K^s, \mathbf{Z}^s, \boldsymbol{\theta}^s)$  be the value of the parameters in step  $s$  of the sampler. Values for parameter  
167  $\boldsymbol{\theta}$  given the block structure can be sampled using any MCMC kernel. In this work, each  $\theta_i$  is  
168 sampled using a random walk on a transformed scale. The difficult proposals are trans-dimensional:  
169 merging and splitting blocks. These are described in the following subsections. The full split-merge  
170 algorithm is given in Algorithm 1.

### 171 *Merge move*

172 The merge proposal takes a state  $(K^s, \mathbf{Z}^s, \boldsymbol{\theta}^s)$  and proposes a new state  $(K', \mathbf{Z}', \boldsymbol{\theta}')$ . Such  
173 a move will reduce the number of blocks by one:  $K' = K^s - 1$ . Firstly, two blocks  $k$  and  $l$   
174 are sampled to merge – possible mechanisms include choosing blocks proportional to block size,  
175 inversely proportional to block size, at random, etc. In this paper, for simplicity, the pair  $k, l$  is  
176 chosen with probability  $1/K^s(K^s - 1)$ . Secondly, the block membership  $\mathbf{Z}'$  is updated. This is  
177 deterministic: any node that is a member of block  $k$  or  $l$  in  $\mathbf{Z}^s$  is assigned to block  $k'$  in  $\mathbf{Z}'$ . All  
178 other nodes keep their block assignment. Next, the parameter values are updated. Following the  
179 recommendations of Green and Richardson (2001), proposing a value  $\boldsymbol{\theta}'_{k'}$  with similar explanatory  
180 power as  $\boldsymbol{\theta}_k$  and  $\boldsymbol{\theta}_l$  should ensure that  $\boldsymbol{\theta}'_{k'}$  is well supported in the posterior. A simple approach  
181 is to take the mean value:  $\boldsymbol{\theta}'_{k'} = \boldsymbol{\theta}_k/2 + \boldsymbol{\theta}_l/2$ ; however, to allow more flexibility in the sampler,  
182 an uneven merge is considered using a weighted mean with tuning parameter  $\lambda \in (0, 1)$ . Since the  
183 split move will invert the merge move, a *matching function*  $m$  is required to ensure that parameters  
184 lie in the correct space. For example, a rate parameter must be positive, whereby a suitable choice  
185 for  $m$  is the exponential function. Possible matching functions for some common parameter spaces  
186 are shown in Table 1. The full parameter proposal during a merge move is shown in Equation (5):

$$187 \quad m(\boldsymbol{\theta}'_{k'}) = \lambda m(\boldsymbol{\theta}_k) + (1 - \lambda) m(\boldsymbol{\theta}_l) \quad (5)$$

---

**Algorithm 1** Reversible jump Markov Chain Monte Carlo sampler for the GSBM with unknown  $K$ : split-merge algorithm.

---

Inputs: edge-weight data  $\mathbf{w}$ , prior parameters  $\boldsymbol{\alpha}, \gamma, \delta$ , sampler parameters  $\lambda, \nu, \sigma$ .

Draw  $K^0, \mathbf{Z}^0 \sim F_0(\cdot | \gamma, \delta)$ .

Draw  $\boldsymbol{\theta}^0 \sim G_0(\cdot | \boldsymbol{\alpha})$ .

**for**  $s = 1, \dots, S$  **do**

    Draw  $\boldsymbol{\theta}^s \sim \text{Update}(\cdot | \mathbf{w}, K^{s-1}, \mathbf{Z}^{s-1}, \boldsymbol{\theta}^{s-1}, \boldsymbol{\alpha})$

    Let  $K^s = K^{s-1}$

**if**  $K^s = 1$  **then**

        Propose a split

**else**

        with probability 1/2 propose a split or a merge

**end if**

**if** There are no empty blocks **then**

        Propose adding an empty block

**else**

        with probability  $\frac{N_\theta}{N_\theta + \nu}$  attempt deleting an empty block.

        or with probability  $\frac{\nu}{N_\theta + \nu}$  attempt adding an empty block.

**end if**

**for**  $i = 1, \dots, N$  **do**

**for**  $k = 1, \dots, K^s$  **do**

            Let  $p_k = g(w_{i\cdot} | \mathbf{Z}_{-i}, Z_{ik} = 1, \boldsymbol{\theta}) f(Z_{ik} = 1 | \mathbf{Z}_{-i})$

**end for**

        Draw  $\mathbf{Z}'_i \sim \text{Multinomial}(\mathbf{p})$

**end for**

    Store sample  $(\mathbf{Z}^s, \boldsymbol{\theta}^s, K^s)$ .

**end for**

**return** samples  $\mathbf{Z}, \boldsymbol{\theta}, K$

---

188 Finally, the acceptance probability  $A_{merge}$  is computed (see [Appendix A](#)) and the next state of the  
 189 sampler  $(K^{s+1}, \mathbf{Z}^{s+1}, \boldsymbol{\theta}^{s+1})$  is taken as  $(K', \mathbf{Z}', \boldsymbol{\theta}')$  with probability  $A_{merge}$ , and as  $(K^s, \mathbf{Z}^s, \boldsymbol{\theta}^s)$   
 190 otherwise.

Table 1: Possible matching functions to ensure parameters lie in the correct space.

Range for $\boldsymbol{\theta}$	Possible matching function $m$
$(\infty, \infty)$	$m(x) = x$
$[0, \infty)$	$m(x) = \log(x)$
$[0, 1]$	$m(x) = \text{logit}(x) = \log(x) - \log(1 - x)$

### 191 *Split move*

192 The split proposal takes a state  $(K^s, \mathbf{Z}^s, \boldsymbol{\theta}^s)$  and proposes a new state  $(K', \mathbf{Z}', \boldsymbol{\theta}')$  with  $K' =$   
 193  $K^s + 1$ . Firstly, the block to split is chosen at random. Possible mechanisms include sampling at  
 194 random among the  $K^s$  blocks, proportional to block size, etc. In this paper the block is chosen  
 195 uniformly amongst the  $K^s$  blocks. To mirror the notation of the merge move, the block to split is  
 196 labelled  $k'$ , and the proposed new blocks  $k$  and  $l$ .

The first step in a split move determines the new block parameters. This requires the inverse  
 of Equation (5). On top of this, an auxiliary variable  $u'$  is needed to match the dimension of the  
 parameter space. In this work,  $u' \sim \text{Normal}(0, \sigma^2)$  and represents the weighted difference of the  
 mapped parameters  $m(\boldsymbol{\theta}_k)$  and  $m(\boldsymbol{\theta}_l)$ . The parameter split is thus:

$$m(\boldsymbol{\theta}_k) = \frac{m(\boldsymbol{\theta}'_{k'}) + u'}{2\lambda'} m(\boldsymbol{\theta}_l) = \frac{m(\boldsymbol{\theta}'_{k'}) - u'}{2(1 - \lambda')}$$

197 Note that the dimension-matching criterion of RJMCMC ([Green, 1995](#)) is achieved since the  
 198 vectors  $(\boldsymbol{\theta}'_{k'}, u', \lambda')$  and  $(\boldsymbol{\theta}_k, \boldsymbol{\theta}_l, \lambda)$  have the same cardinality.

199 To determine  $\mathbf{Z}'$ , the nodes assigned to block  $k'$  in  $\mathbf{Z}^s$  are reassigned to blocks  $k$  and  $l$ . In a  
 200 similar fashion to [Green and Richardson \(2001\)](#), nodes are assigned sequentially to either block  $k$   
 201 or  $l$  proportional to the model likelihood. It is not possible to compute the full likelihood during  
 202 this procedure for the GSBM because edge weights exist between all nodes. Specifically, let  $i$  and  
 203  $j$  be the only nodes in block  $k'$ . Choosing to assign  $i$  to block  $k$  or  $l$  proportional to the likelihood  
 204 requires knowledge of the block membership of  $j$ , which does not yet exist. The quantity can be  
 205 calculated in principle by looking at all the possible allocations of the nodes in block  $k$  to  $k'$  and  
 206  $l'$ . This operation is expensive; instead, it is estimated by the following sequential process:

207 First, all nodes in block  $k'$  are unassigned and placed in a holding set  $\mathcal{I}$ . The set of remaining  
 208 nodes is labelled  $\mathcal{J}$  and the current set of block assignments  $\mathbf{Z}_{\mathcal{J}}$ . Take a permutation  $\sigma(\mathcal{I})$  of  $\mathcal{I}$  –  
 209 this is the order in which nodes will be reassigned to block  $k$  or  $l$ .

When assigning node  $i$ , the following quantity can be calculated:

$$q(Z'_i = k') = \frac{f(\mathbf{w}|Z'_i = k', \mathbf{Z}'_{\mathcal{J}}, \boldsymbol{\theta}')}{f(\mathbf{w}|Z'_i = k', \mathbf{Z}'_{\mathcal{J}}, \boldsymbol{\theta}') + f(\mathbf{w}|Z'_i = l', \mathbf{Z}'_{\mathcal{J}}, \boldsymbol{\theta}')}.$$

210 Node  $i$  is then assigned to block  $k$  with probability  $q(Z'_i = k)$  and to block  $l$  otherwise. Once  
 211 assigned,  $i$  is moved from  $\mathcal{I}$  to  $\mathcal{J}$  for the next assignment.



The total proposal probability of the new block assignment is thus:

$$q(\mathbf{Z}') = \prod_{i \in \sigma(\mathcal{I})} q(Z'_i = k)^{\mathbb{1}[Z'_i = k']} (1 - q(Z'_i = k))^{\mathbb{1}[Z'_i = l']}.$$

212 Finally, the proposed split is accepted as the next state of the sampler with probability  $A_{split}$   
 213 as in Equation (A.1), Appendix A.

#### 214 *Gibbs reassignment move*

215 To allow the sampler to explore the parameter space, an additional two moves are included: a  
 216 Gibbs-like move (which allocates each node to a block proportional to the posterior density) and a  
 217 move that allows the addition and deletion of empty blocks.

218 The Gibbs-like allocation move for node  $i$  computes the conditional posterior value for  $i$  being  
 219 a member of each of the  $K$  blocks in the current state of the sampler. Since  $K$  is finite, this set of  
 220 posterior values can trivially be normalised to a probability vector, such that  $p_{ik}$  is the probability  
 221 that node  $i$  is reassigned to block  $k$ . Thanks to the structure of the GSBM,  $p_{ik}$  can be written as  
 222 the product of two densities: the posterior density of edge weights to nodes in block  $k$ , and the  
 223 posterior density of edge weights to nodes in other blocks:

$$\begin{aligned} p_{ik} &= p(Z_{ik} = 1 | \mathbf{Z}_{-i}, \mathbf{w}, \boldsymbol{\theta}), \\ &\propto f(\mathbf{Z}_{ik} = 1 | \mathbf{Z}_{-i}) \prod_{j \neq i} g(w_{ij} | \mathbf{Z}_j, bZ_{ik} = 1, \boldsymbol{\theta}), \\ &= f(\mathbf{Z}_{ik} = 1 | \mathbf{Z}_{-i}) \prod_{j \neq i} g(w_{ij} | \boldsymbol{\theta}_k)^{Z_{jk}} g(w_{ij} | \boldsymbol{\theta}_0)^{1 - Z_{jk}}. \end{aligned}$$

224 Notice it is possible to reassign  $i$  to its current block. This move, as well as the split move, can  
 225 leave a block empty; waiting for the sampler to merge an empty block with another block can leave  
 226 empty blocks in the sampler state for some time, adding to the uncertainty around the number of  
 227 blocks  $K$ . A proposal that addresses these concerns is considered in the next section.

#### 228 *Add or delete empty blocks*

229 The second extension allows for the deletion and addition of empty blocks; the *delete empty*  
 230 *block* move is the inverse of *add empty block*. During the *delete empty block* move, a candidate  
 231 block is chosen at random from the current set of empty blocks. When an empty block is added,  
 232 it is given the label  $K + 1$ . For simplicity, when an add/delete move is attempted, the probability  
 233 of adding a block is chosen proportional to a sampler parameter  $\nu$ . The probability of choosing to  
 234 delete an empty block is proportional to the number of empty blocks in the current state,  $N_\emptyset$ . Note  
 235 that the likelihood of the edge weights does not change with the addition of empty blocks since the  
 236 entire node structure remains unaffected. When a block is added, a parameter  $\boldsymbol{\theta}^*$  is drawn from  
 237 the prior distribution  $G_0$ . The acceptance probabilities of the add and delete empty block moves  
 238 are calculated as:

$$A_{add} = \frac{\pi_0(K + 1, \mathbf{Z})}{\pi_0(K, \mathbf{Z})} \frac{\nu + N_\emptyset}{\nu(\nu + N_\emptyset + 1)}, \quad \text{and} \quad A_{del} = \frac{\pi_0(K - 1, \mathbf{Z})}{\pi_0(K, \mathbf{Z})} \frac{\nu(\nu + N_\emptyset)}{\nu + N_\emptyset - 1}.$$

239 The sampler is implemented in the R package “SBMSplitMerge” Ludkin (2020). This package  
 240 is used to perform the inference in the following sections.

241 **4. Simulated data**

242 In this section, the split-merge sampler of Section 3 is demonstrated on simulated data. The  
 243 scripts to generate these example networks, run the sampler, and produce the figures (as well as  
 244 the data in Section 5) are available on GitHub ([https://github.com/ludkinm/SBMSplitMerge/](https://github.com/ludkinm/SBMSplitMerge/releases/tag/CRAN-1.1.1)  
 245 [releases/tag/CRAN-1.1.1](https://github.com/ludkinm/SBMSplitMerge/releases/tag/CRAN-1.1.1)).

246 Two data sets are considered. Both consist of 100 nodes split into four blocks with sizes 19,  
 247 23, 27 and 31. Each network has the same block structure. The first data set uses a Bernoulli  
 248 distribution as its edge-weight distribution  $G$ . The second data set uses a generalised negative  
 249 binomial distribution. Data was simulated from the edge-weight distributions with and plotted in  
 250 Figure 1a for the Bernoulli data set, then Figure 2a for the negative binomial.

251 The generalised negative binomial distribution is parameterised by the real-valued “number of  
 252 failures”  $r > 0$  and success probability  $p \in [0, 1]$ . If  $X \sim \text{NegBin}(r, p)$  then:

$$253 \quad \mathbb{P}(X = x) = \frac{\Gamma(x + r)}{\Gamma(r) x!} p^r (1 - p)^x, \text{ for } x = 0, 1, 2, \dots$$

254 Notice that the Bernoulli distribution admits a conjugate prior; therefore, existing samplers, such  
 255 as those introduced by Mørup and Schmidt (2012) and McDaid et al. (2013), could be applied.  
 256 However, for the negative binomial with both  $r$  and  $p$  unknown, no conjugate prior exists.

257 To apply the GSBM, the prior on  $K$  and  $\mathbf{Z}$  was set to a DMA distribution with hyperparameters  
 258 set to  $(\gamma, \delta) = (1, 10)$ . The parameter values used for each of the edge-weight models is given in  
 259 Table 2. For the network with Bernoulli-distributed edge weights, the uniform prior Beta(1, 1) was  
 260 applied to each parameter  $\theta$ . In the negative binomial network with both parameters unknown,  
 261 a Beta(1, 1) distribution is placed on the probability parameter  $p$  and the prior for  $r$  is set to  
 262 Gamma(1, 1).

Table 2: Simulated data parameter values for each edge-weight distribution.

Parameter	$\theta_0$	$\theta_1$	$\theta_2$	$\theta_3$	$\theta_4$
Bernoulli( $p$ )	0.05	0.4	0.5	0.6	0.7
Negative binomial( $p, r$ )	(0.5, 1)	(0.5, 1)	(0.5, 4)	(0.5, 5)	(0.5, 6)

263 In both cases, a random walk Metropolis-Hastings step was applied to  $\theta$  on a transformed  
 264 scale with standard-deviation 0.1. A draw from the prior was taken as the initial state then the  
 265 split-merge sampler of Section 3 ran for 10,000 iterations with 5000 iterations discarded as burn-in.

266 To evaluate the performance of the algorithm, the ability to detect the true number of blocks,  
 267 block structure and parameter values are considered. To measure the ability to detect block struc-  
 268 ture, the posterior joint probabilities that two nodes belong to the same block are calculated after  
 269 burn-in, via:

$$270 \quad P_{ij} = \frac{1}{|\mathcal{S}|} \sum_{s \in \mathcal{S}} \mathbb{I}[Z_{is} = Z_{js}], \quad (6)$$

271 where  $\mathcal{S}$  contains the indices of samples remaining after burn-in.

272 The parameter estimates can be compared to the true values in Table 2. Note that the model in  
 273 Equation (4) is invariant to a permutation of the block labels; this implies that the true and inferred  
 274 structure may be the same up to a permutation of the block labels. To correct for this phenomenon,  
 275 a permutation of the modal block labels under the MCMC to the true labels is derived and applied

276 to the parameters and block labels in the Markov chain (Details are given in [Appendix B](#)). Note  
 277 this matching is only required to compare the true parameter values to the MCMC output.

278 The posterior joint probability that two nodes are in the same block (after burn-in) is displayed  
 279 for the Bernoulli network in [Figure 1b](#). This matches the truth very well: nodes who truly are in  
 280 the same block have high posterior probability of being assigned to the same block ([Equation 6](#)),  
 281 and nodes who are not in the same block have low posterior probability. The trace plot for  $K$  shows  
 282 that for most iterations the sampler had four blocks, matching the truth, but explored some states  
 283 with five or six blocks. The posterior modes of the parameters, and the 5% and 95% posterior  
 284 confidence intervals are shown in [Table 3](#). The posterior modes are all close to the true values in  
 285 [Table 2](#) for the Bernoulli network.

286 For the negative binomial network, [Figure 2b](#) shows that blocks 2, 3 and 4 are well identified  
 287 by the sampler. As for the block 1, recall  $\theta_0 = \theta_1$  in the true parameters; this gives no structure  
 288 to block 1. Indeed, one could reassign the nodes in block 1 arbitrarily between two blocks 1a and  
 289 1b with  $\theta_{1a} = \theta_{1b} = \theta_1$  and the likelihood would be unchanged. (Note this is not true for block  
 290  $k = 2, 3, 4$  since some within-block interactions governed by  $\theta_k \gg \theta_0$  would be governed by  $\theta_0$  under  
 291 such a reassignment.) The sampler is able to explore regions of the posterior where nodes in block  
 292 1 are separate from the other nodes, as seen by the low probability region in the off-diagonal in  
 293 [Figure 2b](#). There is uncertainty around if the nodes in block 1 are in the same block as indicated by  
 294 the range of posterior probabilities in the lower left block of [Figure 2b](#). The estimated parameter  
 295 values in [Table 3](#) lead to similar conclusions: the estimates for parameters  $\theta_0, \theta_2, \theta_3$  and  $\theta_4$  are good,  
 296 but, the poor specification of block 1 leads to poor estimates of  $\theta_1$ .

Table 3: Mode, 5% and 95% posterior quantiles for parameters in example networks.

Model	Bernoulli	Negative Binomial	Negative Binomial
Parameter	$p$	$p$	$r$
$\theta_0$	0.052 (0.046, 0.058)	0.472 (0.442, 0.497)	0.895 (0.801, 0.978)
$\theta_1$	0.425 (0.366, 0.491)	0.436 (0.059, 0.997)	0.642 (0.001, 1.575)
$\theta_2$	0.506 (0.453, 0.557)	0.467 (0.392, 0.536)	3.196 (2.410, 4.126)
$\theta_3$	0.638 (0.598, 0.677)	0.536 (0.472, 0.600)	5.545 (4.330, 7.183)
$\theta_4$	0.678 (0.643, 0.714)	0.477 (0.425, 0.532)	5.392 (4.480, 6.692)

297 Assessing the convergence of a reversible jump Markov chain is non-trivial. Two techniques  
 298 are applied in this section: (i) applying the Gelman-Rubin convergence statistic ([Gelman and](#)  
 299 [Rubin, 1992](#)) to a summary statistic and (ii) starting two independent samplers from extreme block  
 300 configurations – one with all nodes assigned to one block and the other with each node assigned to  
 301 a unique block.

302 In the first case, the mean and variance of the parameter values are used as summary statistics of  
 303 the sampler performance, which are recorded at every iteration of the sampler. The Gelman-Rubin  
 304 statistics for the sampler for each model are shown in [Table 4](#) based on 30 independent chains.  
 305 These values are close to 1, indicating that convergence appears to have occurred during the first  
 306 10,000 iterations.

307 The second technique for assessing convergence is inspired by perfect simulation: starting two  
 308 samplers at opposite extremes of the parameter space and observing both converging to the same  
 309 area of the posterior indicates that the underlying Markov chains have converged. This process was  
 310 used for the simulated data sets; trace plots for the number of blocks in each case are shown in  
 311 [Figure 3](#).

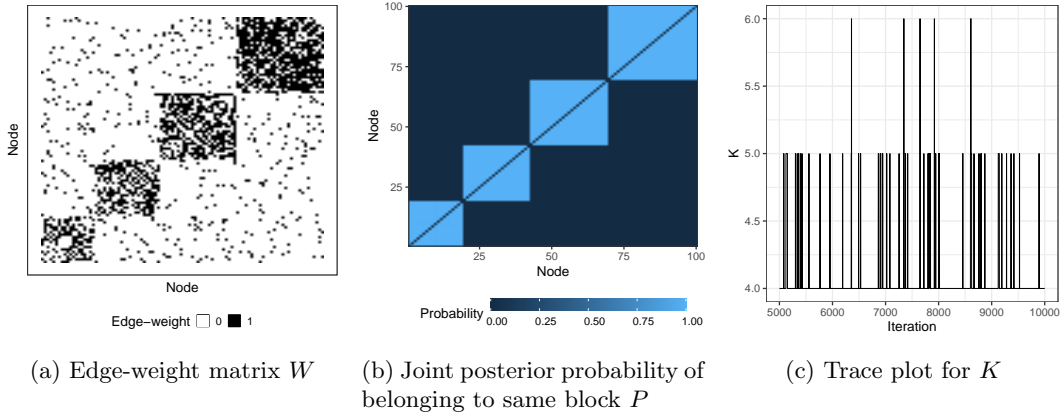


Figure 1: Bernoulli edge weights: adjacency matrix and posterior summaries for block membership and number of blocks  $K$ .

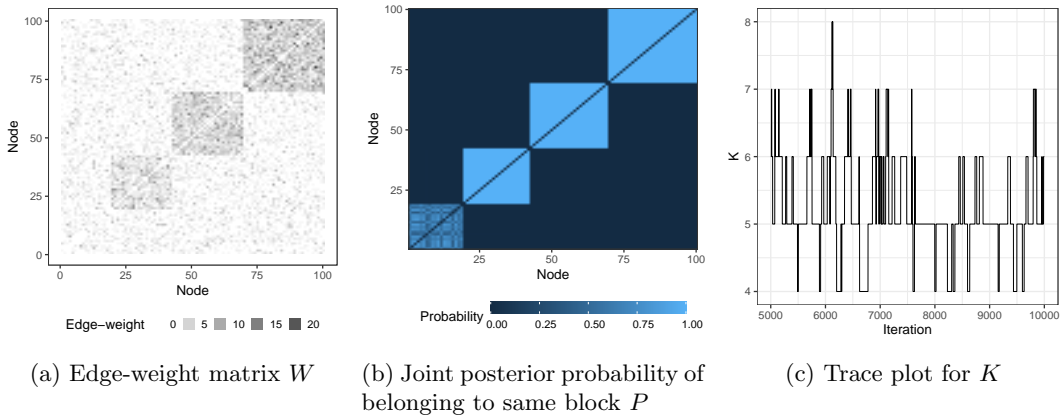


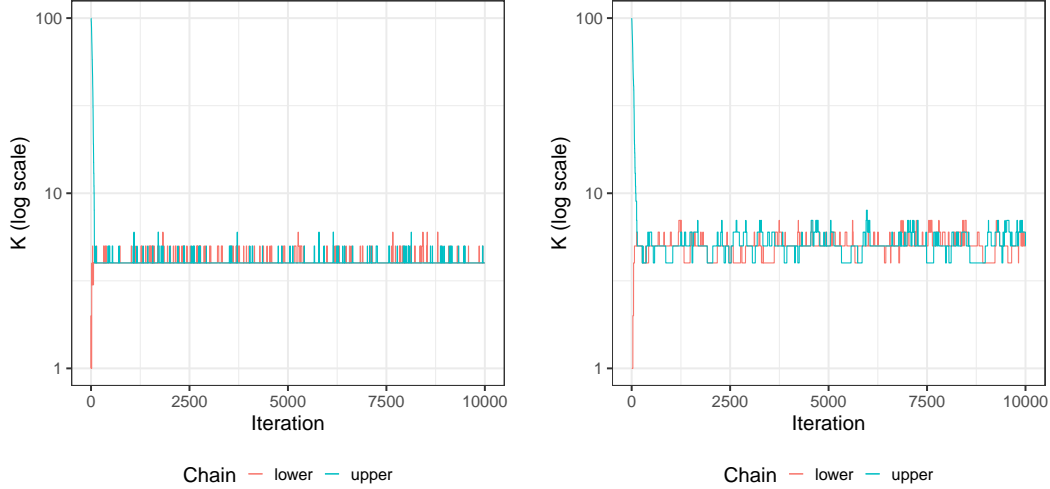
Figure 2: Negative binomial edge weights: adjacency matrix and posterior summaries for block membership and number of blocks  $K$ .

Model	Bernoulli	Negative binomial
Mean	1.0005 (1.0007)	1.0098 (1.0153)
Variance	1.0005 (1.0006)	1.0069 (1.0106)

Table 4: Rubin-Gelman statistics (and upper bound of 95% confidence interval) for each model with 30 independent chains of 10000 iterations.

312 **5. Real data**

313     The split-merge sampler is demonstrated on real networks: a network of brain connectivity with  
 314 binary edge weights in Section 5.1 and a network of emails with count data for edge weights in  
 315 Section 5.2.



(a) Bernoulli: Perfect simulation trace plot for  $K$  (b) Negative binomial: Perfect simulation trace plot for  $K$

Figure 3: Trace plots for number of blocks  $K$  in example networks. Two chains are simulated in each case: the “lower chain” with all nodes initially in one block (orange line) and the “upper chain” with all nodes initially assigned to different blocks (teal line).

### 316 5.1. Macaque sensory data

317 The first data set analysed concerns the brain of a macaque monkey (Négyessy et al., 2006).  
 318 Regions of the cortex were deemed connected, or not, during a sensory task. In total, 45 regions of  
 319 the brain were analysed as a network.

320 A block model was proposed to partition the regions of the brain. This model assigns regions of  
 321 the brain to the same block if their neural activity is similar. Since the data only provides binary  
 322 edge weights, a Bernoulli-SBM is applied. A Beta(1,1) prior was placed on the edge probability  
 323 parameters  $\theta_k$  and a DMA(1,6) prior is placed on  $(K, \mathbf{Z})$  for the block structure, thus the prior  
 324 expected number of blocks is five. The split-merge algorithm was run for 10,000 iterations to  
 325 provide samples from the posterior distribution of both block membership and parameter values.  
 326 1500 samples were discarded as burn-in.

327 Figure 4 displays posterior summaries for the split-merge sampler. A trace plot for the number  
 328 of blocks,  $K$ , is shown in Figure 4c. This shows that the sampler settles on between four and six  
 329 blocks with mode five. The joint posterior probability matrix  $P$  was calculated using Equation (6)  
 330 and the modal block assignments were calculated from the MCMC chain output. Using the modal  
 331 assignments, the nodes are ordered by block label. This ordering applied to the edge-weight matrix  
 332  $W$  and  $P$  are shown in Figure 4a and 4b respectively. The five blocks can be seen in Figure 4b  
 333 as shown by the light blue regions. Counting from the lower left of Figure 4b, block five consists  
 334 of two nodes; these nodes also have some probability of belonging to block three, as indicated by  
 335 the shading in the final two columns/rows. Similarly, some uncertainty is displayed in the block  
 336 membership of the first nodes in blocks three and four. Modal parameter estimates are shown in  
 337 Table 5 together with 5% and 95% quantiles and the effective sample size. The parameters for  
 338 smaller blocks have wider confidence intervals; this is expected since there are fewer edge weights

339 governed by those parameters. Note that parameter  $\theta_5$  is more uncertain; this is due to the block  
 340 consisting of two nodes, meaning that  $\theta_5$  only governs one edge weight. The effective sample size  
 341 cannot be computed for this parameter since it is absent in many iterations when the block has  
 342 been merged with another block.

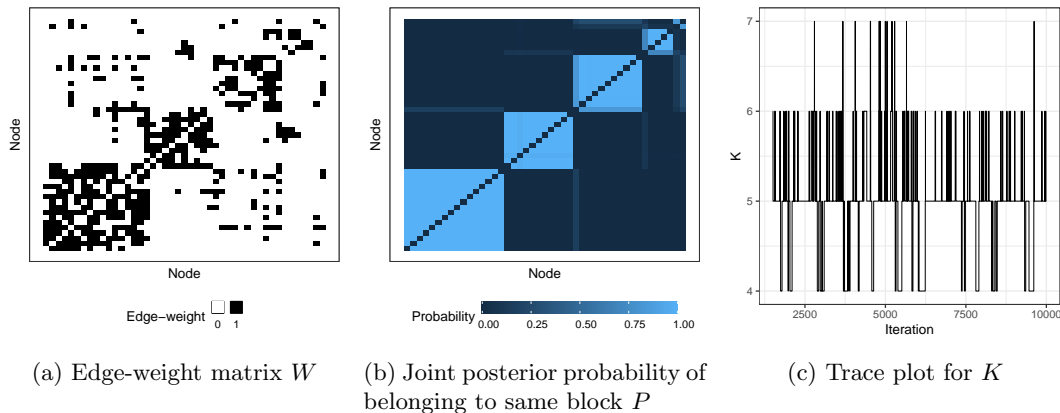


Figure 4: Posterior summaries for block membership in macaque brain network ordered by modal block assignments.

Table 5: Modal parameter estimates, 95% posterior quantiles and effective sample sizes for macaque network.

Parameter	Mode	5%	95%	Effective sample size
$\theta_0$	0.09	0.08	0.11	1048
$\theta_1$	0.70	0.64	0.75	553
$\theta_2$	0.72	0.63	0.80	251
$\theta_3$	0.56	0.43	0.68	126
$\theta_4$	0.58	0.36	0.82	71
$\theta_5$	0.70	0.15	0.99	NA

### 343 5.2. Enron emails

344 The Enron corporation was declared bankrupt in 2001 and later multiple employees were found  
 345 guilty of accounting fraud. As a result of the trial, a corpus of emails leading up to the closure  
 346 of the company was released as a public data set (Klimt and Yang, 2004). Aggregate counts of  
 347 emails between any two employees are arranged into an edge-weight matrix. Note that this network  
 348 contains directed edges and self-loops (since some emails are sent to mailing lists, to which the sender  
 349 belongs). Two models for the edge weights were considered for this model: (i) a Poisson with a  
 350 Gamma(1,1) prior and (ii) a negative binomial with a Gamma(1,1) prior for  $r$  and a Beta(1,1) prior  
 351 for  $p$ . In both cases a DMA(1,10) joint prior is placed on  $K, \mathbf{Z}$ . On a first analysis, the mean  
 352 number of emails sent by any one employee is 3.7, whilst the variance is 4753, so a Poisson model  
 353 seems a bad fit *a priori*. The split-merge algorithm of Section 3 was applied with 10,000 iterations  
 354 and 1500 discarded as burn-in.

355 As in Section 5.1, the joint posterior probability matrix  $P$  was calculated using Equation (6)  
 356 and the modal block assignments were calculated from the MCMC chain output. Using the modal

357 assignments, the nodes are ordered by block label. This ordering applied to the log edge-weight  
 358 matrix  $W$  and  $P$  in Figure 5a and Figure 5b respectively. The negative binomial model is more  
 359 flexible and is thus able to more easily detect structure in the network compared to the Poisson  
 360 model. This is exemplified in the ordered plot of the log edge weights in Figures 5a and 6a.  
 361 Furthermore, the fit using the Poisson distribution for edge weights finds one large group (fourth  
 362 from the left in Figure 5b) with a low incidence of sent emails. This group corresponds to parameter  
 363  $\lambda_4$ , which has a posterior mode of 0.19. Under the negative binomial distribution, the low-incidence  
 364 group is much smaller, with modal parameters  $r_9 = 0.004$  and  $p_9 = 0.012$  giving an expected number  
 365 of emails sent by a node in block nine as  $r(1-p)/p \simeq 0.33$ . The modal parameter values for each  
 366 model are given in Table 6 together with the 5% and 95% quantiles.

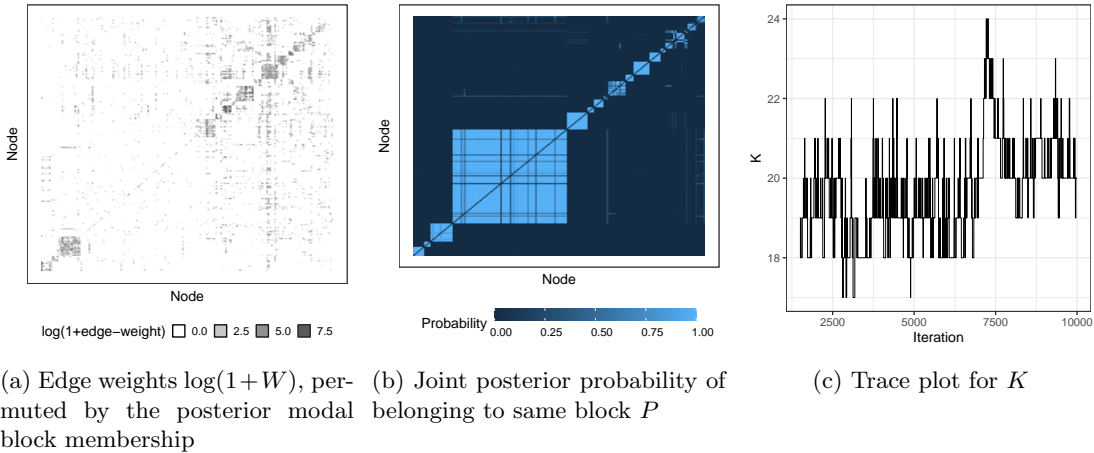


Figure 5: Posterior summaries for block membership in Enron network with Poisson edge-weight model (after burn-in).

## 367 6. Concluding remarks

368 This paper considered a generalisation of the stochastic block model by allowing arbitrary edge-  
 369 weight distributions and explicitly modelling the number of blocks. A Bayesian inference algorithm  
 370 was proposed: a split-merge reversible jump Markov chain Monte Carlo sampler as described in  
 371 Section 3. Unlike previous Bayesian treatments of the stochastic block model with an unknown  
 372 number of blocks (Mørup and Schmidt, 2012, 2013; McDaid et al., 2013), the proposed algorithm  
 373 handles edge-weight distributions without conjugate priors. This allows for more flexible modelling  
 374 of network data, as demonstrated in Section 5.2 on the Enron email network. In this example, a  
 375 negative binomial model (with both parameters unknown) was fit to the edge weights, allowing  
 376 for a higher variance of edge weights within a block than under the Poisson model. In the Enron  
 377 data set, the negative binomial explored the parameter space better than the Poisson model since  
 378 it visited posterior states with more structure.

379 The algorithm presented here is general and can be applied to the generalised stochastic block  
 380 model with any edge-weight distributions from which samples can be taken and densities evaluated.  
 381 This can easily include co-variate information in either the edge-weight distribution,  $G$ , or the block  
 382 membership distribution,  $F$ .

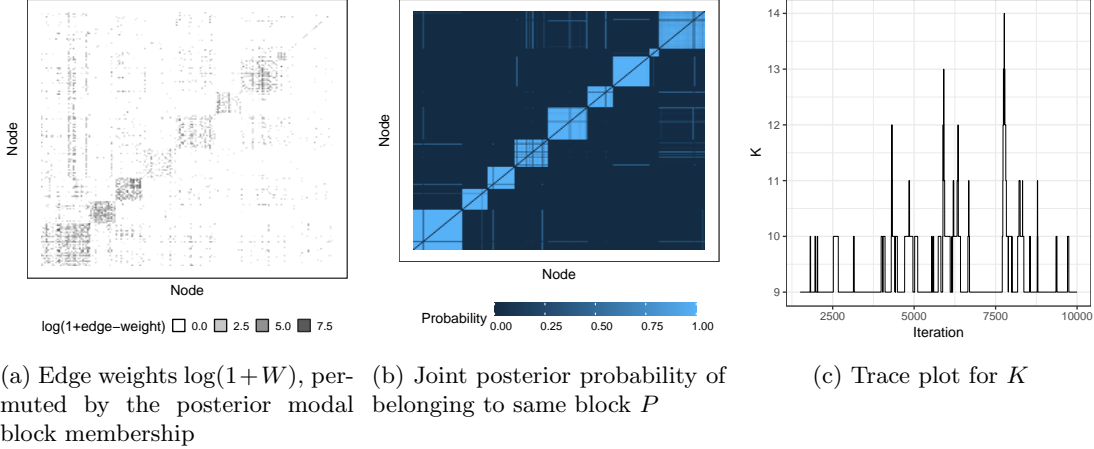


Figure 6: Posterior summaries for block membership in Enron network with negative binomial edge-weight model (after burn-in).

383 For simplicity, the models presented in Section 2 assume all edges are present in the network  
 384 and that each edges has a recorded edge weight. This assumption can be relaxed in (at least) two  
 385 ways. Firstly, if some set of edges  $\mathcal{A}$  is known to be absent from the network, then the set of  
 386 edges is  $\mathcal{E}_A = \mathcal{E}/\mathcal{A}$ . For example, consider a network of electrical cables between substations. The  
 387 substations are represented by nodes, the cables by edges and the voltage along a cable by an edge  
 388 weight. In this case, Equation 2 remains unchanged except the last line runs over all  $ij \in \mathcal{E}_A$  rather  
 389 than  $\mathcal{E}$ . To adapt the split-merge sampler, the likelihood calculations involving node  $i$  iterate over  
 390 all nodes  $j \in \mathcal{E}_A/\{i\}$  instead of all  $i \neq j$ . In the second case, the edge exists in the model but the  
 391 edge weight is not recorded in the data set; this is a missing data problem. Two approaches are  
 392 possible: either the edge weight was not recorded, or the edge does not exist. In the first case, one  
 393 could use a data augmentation scheme within the split-merge sampler to infer the state of missing  
 394 edge weights. In the second case, a sparsity parameter as in Matias and Miele (2017) could be  
 395 inferred within the GSBM framework. This treats edge weights as a mixture of the density  $G$  and  
 396 a Dirac mass at zero representing the non-existence of an edge.

### 397 Acknowledgements

398 The author would like to thank the referees as well as Brendan Murphy, Simon Lunagomez  
 399 and Peter Neal for helpful comments. Funding: This work was supported by the Engineering and  
 400 Physical Sciences Research Council (EPSRC) [EP/H023151/1 and EP/P033075/1].

### 401 Appendix A. Acceptance probability calculations

402 Since a merge move is the inverse of a split move,  $A_{merge} = 1/A_{split}$ , hence only  $A_{split}$  is derived.  
 403 The acceptance probability can be split into the following parts: posterior density ratio, proposal  
 404 density ratio, ratio of densities of auxiliary variables, and the Jacobian; as such  $A_{split}$  has the



Table 6: Parameter mode, 5% and 95% posterior quantiles for the Enron data with edge-weight model: (i) Poisson( $\lambda$ ) and (ii) NegativeBinomial( $r, p$ )

$\theta$	Mode	5%	95%
$r_0$	0.012	0.011	0.012
$r_1$	0.133	0.122	0.147
$r_2$	0.323	0.282	0.374
$r_3$	0.169	0.149	0.194
$r_4$	0.086	0.069	0.106
$r_5$	0.082	0.070	0.100
$r_6$	0.114	0.092	0.139
$r_7$	0.120	0.104	0.137
$r_8$	0.460	0.259	0.706
$r_9$	0.004	0.002	0.022
$p_0$	0.013	0.012	0.015
$p_1$	0.003	0.002	0.003
$p_2$	0.007	0.006	0.009
$p_3$	0.002	0.002	0.003
$p_4$	0.020	0.014	0.029
$p_5$	0.007	0.005	0.010
$p_6$	0.008	0.005	0.011
$p_7$	0.006	0.005	0.008
$p_8$	0.039	0.019	0.064
$p_9$	0.012	0.001	0.041
$\lambda_0$	1.45	1.39	1.50
$\lambda_1$	43.67	41.49	45.29
$\lambda_2$	32.43	30.33	34.70
$\lambda_3$	52.62	51.69	57.98
$\lambda_4$	0.19	0.15	0.23
$\lambda_5$	30.28	27.15	31.14
$\lambda_6$	146.85	142.71	151.71
$\lambda_7$	498.32	492.65	505.24
$\lambda_8$	29.51	20.73	174.72
$\lambda_9$	161.93	23.59	343.92

405 general form:

$$\begin{aligned}
 A_{split} &= \frac{\pi(\kappa + 1, \mathbf{z}', \boldsymbol{\theta}' | E)}{\pi(\kappa, \mathbf{z}, \boldsymbol{\theta} | E)} \frac{q(\kappa, \mathbf{z}, \boldsymbol{\theta} | \kappa + 1, \mathbf{z}', \boldsymbol{\theta}')}{q(\kappa + 1, \mathbf{z}', \boldsymbol{\theta}' | \kappa, \mathbf{z}, \boldsymbol{\theta})} \frac{q(\lambda)}{q(u', \lambda')} J_{split} \\
 &= \frac{\pi(\kappa + 1, \mathbf{z}', \boldsymbol{\theta}' | E)}{\pi(\kappa, \mathbf{z}, \boldsymbol{\theta} | E)} \frac{q(merge | \kappa + 1)}{q(split | \kappa)} \frac{q(k', l')}{q(k)} \frac{q(\lambda)}{q(\lambda', u')} \frac{1}{q(\mathbf{z}' | \boldsymbol{\theta}')} J_{split}
 \end{aligned}
 \tag{A.1}$$

407 where  $q(split | \kappa)$  and  $q(merge | \kappa)$  are the probabilities of proposing a split or merge move given that  
408 the current state of the sampler contains  $\kappa$  blocks. These are chosen as 1/2 where possible. That  
409 is  $q(split | \kappa = 1) = 1$  and  $q(merge | \kappa = 1) = 0$  since merging is impossible when there is only one  
410 block. Note that in the examples:  $\lambda, \lambda' \stackrel{iid}{\sim} \text{Unif}(0, 1)$ ,  $u' \sim \text{Normal}(0, 1)$ ,  $k'$  and  $k, l$  are sampled at

411 random amongst the set of available blocks.

412 Finally,  $J_{split}$  is the Jacobian of the split proposal given in Equation (A.2) and  $p$  is the dimen-  
 413 sionality of each  $\theta_k$ .

$$414 \quad J_{split} = \begin{vmatrix} \frac{\partial \theta'_{k'}}{\partial \theta_k} & \frac{\partial \theta'_{l'}}{\partial \theta_k} \\ \frac{\partial \theta'_{k'}}{\partial u'} & \frac{\partial \theta'_{l'}}{\partial u'} \end{vmatrix} = \left| \frac{\nabla \mathbf{m}(\theta'_{k'}) \nabla \mathbf{m}(\theta'_{l'})}{\nabla \mathbf{m}(\theta_k) (2\lambda(1-\lambda))^p} \right| \quad (\text{A.2})$$

Therefore, in the examples, where specific choices for  $u'$ ,  $\lambda'$ ,  $\lambda$  and  $q(\text{merge})$ ,  $q(\text{split})$  have been made, the acceptance probabilities reduce to:

$$\begin{aligned} A_{split} &= \frac{\pi(\kappa + 1, \mathbf{z}', \theta' | E)}{\pi(\kappa, \mathbf{z}, \theta | E)} \frac{1}{1 + \mathbb{I}[\kappa = 1]} \frac{2}{\kappa + 1} \\ &\quad \times \frac{1}{\phi(u' | 0, \sigma^2)} \frac{1}{q(\mathbf{z}' | \theta')} \left| \frac{\nabla \mathbf{m}(\theta'_{k'}) \nabla \mathbf{m}(\theta'_{l'})}{\nabla \mathbf{m}(\theta_k) (2\lambda(1-\lambda))^p} \right| \\ A_{merge} &= \frac{\pi(\kappa - 1, \mathbf{z}', \theta' | E)}{\pi(\kappa, \mathbf{z}, \theta | E)} (1 + \mathbb{I}[\kappa = 2]) \frac{\kappa}{2} \\ &\quad \times \phi(u | 0, \sigma^2) q(\mathbf{z} | \theta) \left| \frac{\nabla \mathbf{m}(\theta'_{k'}) (2\lambda(1-\lambda))^p}{\nabla \mathbf{m}(\theta_k) \nabla \mathbf{m}(\theta_l)} \right| \end{aligned}$$

## 415 Appendix B. Post-hoc matching

416 The GSBM is invariant to relabelling of the nodes – Equation 4 gives the same posterior value  
 417 if the node labels are permuted. This causes a problems when comparing the output of the MCMC  
 418 against some known parameter values in Section 4, since the estimated block labels need to match  
 419 the truth for a reasonable comparison.

Let  $Z^{\text{true}}$  be a set of true block labels. We match the MCMC output labels to the true labels by matching the modal assignment vector  $Z^{\text{mode}}$  to  $Z^{\text{true}}$ , where

$$Z_i^{\text{mode}} = \arg \max_k \sum_{\mathcal{S}} \mathbb{I}[Z_{is} = k],$$

420 gives the most-often used block label for node  $i$  during the MCMC iterations in  $\mathcal{S}$ .

Given  $Z^{\text{true}}$  and  $Z^{\text{mode}}$ , a contingency table  $n$  is formed via:

$$n_{ck} = \sum_i \mathbb{I}[(Z_i^{\text{mode}} = c) \& (Z_i^{\text{true}} = k)].$$

421 Thus entry  $c, k$  in the table is the number of nodes assigned to block  $c$  under the mode and block  
 422  $k$  under the truth.

423 Let  $\pi$  be a permutation with  $\pi_c = \arg \max_k n_{ck}$ . We relabel the MCMC output for each  
 424  $i = 1, \dots, N$  and  $s \in \mathcal{S}$  via  $Z_{is} = c \mapsto Z_{is} = \pi_c$  and  $\theta_c \mapsto \theta_{\pi_c}$ . Under this relabelling the modal and  
 425 true labels match so comparisons between parameters can be made.

426 **References**

- 427 Airoldi, E. M., Blei, D. M., Fienberg, S. E., Xing, E. P., 2008. Mixed membership stochastic  
428 blockmodels. *Journal of Machine Learning Research* 9 (Sep), 1981–2014.
- 429 Ambroise, C., Matias, C., 2012. New consistent and asymptotically normal parameter estimates  
430 for random-graph mixture models. *Journal of the Royal Statistical Society: Series B (Statistical  
431 Methodology)* 74 (1), 3–35.
- 432 Chen, K., Lei, J., 2016. Network cross-validation for determining the number of communities in  
433 network data. *Journal of the American Statistical Association*, 1–11.  
434 URL <https://doi.org/10.1080/01621459.2016.1246365>
- 435 Copic, J., Jackson, M. O., Kirman, A., 2009. Identifying community structures from network data  
436 via maximum likelihood methods. *The BE Journal of Theoretical Economics* 9 (1).
- 437 Daudin, J.-J., Picard, F., Robin, S., 2008. A mixture model for random graphs. *Statistics and  
438 Computing* 18 (2), 173–183.  
439 URL <https://doi.org/10.1007/s11222-007-9046-7>
- 440 Fienberg, S. E., Meyer, M. M., Wasserman, S. S., 1985. Statistical analysis of multiple sociometric  
441 relations. *Journal of the American Statistical Association* 80 (389), 51–67.
- 442 Frank, O., Harary, F., 1982. Cluster inference by using transitivity indices in empirical graphs.  
443 *Journal of the American Statistical Association* 77 (380), 835–840.
- 444 Gelman, A., Rubin, D. B., 1992. Inference from iterative simulation using multiple sequences.  
445 *Statist. Sci.* 7 (4), 457–472.  
446 URL <https://doi.org/10.1214/ss/1177011136>
- 447 Geng, J., Bhattacharya, A., Pati, D., 2019. Probabilistic community detection with unknown num-  
448 ber of communities. *Journal of the American Statistical Association* 114 (526), 893–905.
- 449 Gershman, S. J., Blei, D. M., 2012. A tutorial on Bayesian nonparametric models. *Journal of  
450 Mathematical Psychology* 56 (1), 1 – 12.  
451 URL <https://doi.org/10.1016/j.jmp.2011.08.004>
- 452 Green, P. J., 1995. Reversible jump Markov chain Monte Carlo computation and Bayesian model  
453 determination. *Biometrika* 82 (4), 711–732.
- 454 Green, P. J., Richardson, S., 2001. Modelling heterogeneity with and without the Dirichlet process.  
455 *Scandinavian Journal of Statistics* 28 (2), 355–375.  
456 URL <http://dx.doi.org/10.1111/1467-9469.00242>
- 457 Hoff, P. D., Raftery, A. E., Handcock, M. S., 2002. Latent space approaches to social network  
458 analysis. *Journal of the American Statistical Association* 97 (460), 1090–1098.  
459 URL <https://doi.org/10.1198/016214502388618906>
- 460 Holland, P. W., Laskey, K. B., Leinhardt, S., 1983. Stochastic blockmodels: First steps. *Social  
461 networks* 5 (2), 109–137.

- 462 Jiang, Q., Zhang, Y., Sun, M., 2009. Community detection on weighted networks: A variational  
463 Bayesian method. In: Asian Conference on Machine Learning. Springer, pp. 176–190.
- 464 Karrer, B., Newman, M. E., 2011. Stochastic blockmodels and community structure in networks.  
465 Physical Review E 83 (1), 016107.
- 466 Kemp, C., Tenenbaum, J. B., Griffiths, T. L., Yamada, T., Ueda, N., 2006. Learning systems of  
467 concepts with an infinite relational model. In: AAAI. Vol. 3. p. 5.
- 468 Kliment, B., Yang, Y., 2004. Machine Learning: ECML 2004: 15th European Conference on Machine  
469 Learning, Pisa, Italy, September 20-24, 2004. Proceedings. Springer Berlin Heidelberg, Berlin,  
470 Heidelberg, Ch. The Enron Corpus: A New Dataset for Email Classification Research, pp. 217–  
471 226.
- 472 Latouche, P., Birmele, E., Ambroise, C., 2012. Variational Bayesian inference and complexity con-  
473 trol for stochastic block models. Statistical Modelling 12 (1), 93–115.
- 474 Lei, J., 2016. A goodness-of-fit test for stochastic block models. The Annals of Statistics 44 (1),  
475 401–424.  
476 URL <https://doi.org/10.1214/15-aos1370>
- 477 Ludkin, M., 2020. SBMSplitMerge: Inference for a Generalised SBM with a Split Merge Sampler.  
478 R package version 1.1.1.  
479 URL <https://cran.r-project.org/package=SBMSplitMerge>
- 480 Ludkin, M., Eckley, I., Neal, P., 2018. Dynamic stochastic block models: parameter estimation and  
481 detection of changes in community structure. Statistics and Computing.  
482 URL <https://doi.org/10.1007/s11222-017-9788-9>
- 483 Mariadassou, M., Robin, S., Vacher, C., 2010. Uncovering latent structure in valued graphs: a  
484 variational approach. The Annals of Applied Statistics, 715–742.
- 485 Matias, C., Miele, V., 2017. Statistical clustering of temporal networks through a dynamic stochastic  
486 block model. Journal of the Royal Statistical Society: Series B (Statistical Methodology) 79 (4),  
487 1119–1141.
- 488 Matias, C., Robin, S., 2014. Modeling heterogeneity in random graphs through latent space models:  
489 a selective review. ESAIM: Proc. 47, 55–74.  
490 URL <https://doi.org/10.1051/proc/201447004>
- 491 McDaid, A. F., Murphy, T. B., Friel, N., Hurley, N. J., 2013. Improved Bayesian inference for  
492 the stochastic block model with application to large networks. Computational Statistics & Data  
493 Analysis 60, 12–31.  
494 URL <http://dx.doi.org/10.1016/j.csda.2012.10.021>
- 495 Miller, J. W., Harrison, M. T., 2018. Mixture models with a prior on the number of components.  
496 Journal of the American Statistical Association 113 (521), 340–356.
- 497 Mørup, M., Schmidt, M. N., 2012. Bayesian community detection. Neural computation 24 (9),  
498 2434–2456.

- 499 Mørup, M., Schmidt, M. N., 2013. Nonparametric Bayesian modeling of complex networks: an  
500 introduction. *IEEE Signal Processing Magazine* 30 (3), 110–128.
- 501 Mørup, M., Schmidt, M. N., Hansen, L. K., 2011. Infinite multiple membership relational mod-  
502 eling for complex networks. In: *Machine Learning for Signal Processing (MLSP), 2011 IEEE*  
503 *International Workshop on.* IEEE, pp. 1–6.
- 504 Négyessy, L., Nepusz, T., Kocsis, L., Bazsó, F., 2006. Prediction of the main cortical areas and  
505 connections involved in the tactile function of the visual cortex by network analysis. *European*  
506 *Journal of Neuroscience* 23 (7), 1919–1930.
- 507 Nobile, A., Fearnside, A. T., 2007. Bayesian finite mixtures with an unknown number of components:  
508 The allocation sampler. *Statistics and Computing* 17 (2), 147–162.  
509 URL <https://doi.org/10.1007/s11222-006-9014-7>
- 510 Nowicki, K., Snijders, T. A. B., 2001. Estimation and prediction for stochastic blockstructures.  
511 *Journal of the American Statistical Association* 96 (455), 1077–1087.  
512 URL <https://doi.org/10.1198/016214501753208735>
- 513 Peixoto, T. P., 2013. Parsimonious module inference in large networks. *Physical Review Letters*  
514 110 (14).  
515 URL <https://doi.org/10.1103/physrevlett.110.148701>
- 516 Saldaña, D. F., Yu, Y., Feng, Y., 2017. How many communities are there? *Journal of Computational*  
517 *and Graphical Statistics* 26 (1), 171–181.  
518 URL <https://doi.org/10.1080/10618600.2015.1096790>
- 519 Snijders, T. A., Nowicki, K., 1997. Estimation and prediction for stochastic blockmodels for graphs  
520 with latent block structure. *Journal of classification* 14 (1), 75–100.
- 521 Snijders, T. A. B., Pattison, P. E., Robins, G. L., Handcock, M. S., 2006. New specifications for  
522 exponential random graph models. *Sociological Methodology* 36 (1), 99–153.
- 523 Wang, Y. R., Bickel, P. J., et al., 2017. Likelihood-based model selection for stochastic block models.  
524 *The Annals of Statistics* 45 (2), 500–528.
- 525 Wasserman, S., Anderson, C., 1987. Stochastic a posteriori blockmodels: Construction and assess-  
526 ment. *Social Networks* 9 (1), 1–36.  
527 URL [https://doi.org/10.1016/0378-8733\(87\)90015-3](https://doi.org/10.1016/0378-8733(87)90015-3)
- 528 Xin, L., Zhu, M., Chipman, H., 2017. A continuous-time stochastic block model for basketball  
529 networks. *The Annals of Applied Statistics* 11 (2), 553–597.